



King's Research Portal

DOI:

[10.1109/GLOCOM.2016.7842119](https://doi.org/10.1109/GLOCOM.2016.7842119)

Document Version

Peer reviewed version

[Link to publication record in King's Research Portal](#)

Citation for published version (APA):

Al-Kadri, M. O., Deng, Y., & Nallanathan, A. (2017). Outage probability of heterogeneous cellular networks with full-duplex small cells. In 2016 IEEE Global Communications Conference, GLOBECOM 2016 - Proceedings [7842119] Washington D.C, USA: IEEE. <https://doi.org/10.1109/GLOCOM.2016.7842119>

Citing this paper

Please note that where the full-text provided on King's Research Portal is the Author Accepted Manuscript or Post-Print version this may differ from the final Published version. If citing, it is advised that you check and use the publisher's definitive version for pagination, volume/issue, and date of publication details. And where the final published version is provided on the Research Portal, if citing you are again advised to check the publisher's website for any subsequent corrections.

General rights

Copyright and moral rights for the publications made accessible in the Research Portal are retained by the authors and/or other copyright owners and it is a condition of accessing publications that users recognize and abide by the legal requirements associated with these rights.

- Users may download and print one copy of any publication from the Research Portal for the purpose of private study or research.
- You may not further distribute the material or use it for any profit-making activity or commercial gain
- You may freely distribute the URL identifying the publication in the Research Portal

Take down policy

If you believe that this document breaches copyright please contact librarypure@kcl.ac.uk providing details, and we will remove access to the work immediately and investigate your claim.

Outage Probability of Heterogeneous Cellular Networks with Full-Duplex Small Cells

M. Omar Al-Kadri*, Yansha Deng*, and Arumugam Nallanathan*

*Department of Informatics, King's College London, UK

Abstract—Full-duplex (FD) small cells provide a promising solution for meeting the sought requirements of future wireless networks, specifically, the capacity, coverage and spectral efficiency. Motivated by the recent developments in self-interference (SI) cancellation techniques, the main objective of this paper is to further investigate the impact of using fully FD-capable small cells on conventional HetNets. We analyse a two-tier heterogeneous cellular networks (HetNets), wherein tier 1 consists of legacy half-duplex (HD) macro base stations (BSs) while tier 2 consists of FD small cells. Based on the stochastic geometry approach, we develop a theoretical model and derive closed-form expressions for the outage probability of downlink macrocell users, in addition to downlink and uplink users of small cells since they operate in FD mode. Analytical and simulation results are provided to verify the derived expressions and evaluate the variation of different parameters on the network performance.

I. INTRODUCTION

Full-Duplex (FD) systems are prone to self-interference (SI), which is the interference generated by the transmitter of the device on its own receiver. In the past, FD systems could not be realized due to the inefficiency of SI cancellation techniques [1]. However, recent advances in SI cancellation techniques [2]–[4] have made the in-band FD wireless systems feasible for wireless communications. The in-band FD technology not only offers the potential of doubling the capacity and the spectrum utilization, but also assists in solving some of the key problems in HD systems, such as the hidden node issues, loss of throughput due to high congestion rates, and large end-to-end delays [5].

On the other hand, small cells were proposed as an easy and cost-efficient solution to achieve higher capacity and broader coverage compared with macro-centric networks [6], [7]. It has attracted increasing attention for the fifth generation (5G) wireless communication. The low transmit power characteristic of small cells makes them an ideal candidate for deployment of FD technology, since SI at the small cell BS is easier to control compared to their high-powered macro counterparts. This motivates the research on performance gains of using FD small cells in heterogeneous cellular networks (HetNets).

In existing literature, research on FD network analysis has been carried out. In [8], the authors have analyzed the sum ergodic capacity of interference coordinated HetNets comprising single HD macrocell and single FD-enabled small cell. A comparison between the performance of HD and FD small cell is also provided. In [9], the authors have considered hybrid duplex heterogeneous networks composed of multi-tier networks, with access points operating either in bi-directional FD mode

or downlink HD mode, where the throughput expression was derived. Their results have shown that having tiers with hybrid duplex access points degrades the performance, while higher throughput was achieved when each tier operates in a specific mode, either HD or FD rather than a mixture of both, which motivated further research on full HD operating BSs in tier 1 and full FD operating BSs in tier 2 instead of considering hybrid scenarios. In [10], the closed-form expressions for the outage probability, average ergodic rate, and the minimum average user throughput were derived for a downlink HD multi-tier networks. They have also concluded that neither the number of BSs nor tiers affect outage probability or average ergodic rate in an interference-limited full-loaded HetNet with unbiased cell association. These conclusions, however, may not hold in environments which are prone to higher SI, for instance, HetNets comprising of FD nodes. In [11], a framework is proposed to model the downlink rate coverage probability of a user in a fully FD small cell network with massive MIMO wireless backhauls. Moreover, some recent studies have investigated outage probability of FD relay networks [12]. However, research on outage analysis of HetNets with FD tier, using tools of stochastic geometry, have not been done before and motivates this study.

Unlike previous studies, the main contribution of this paper is to investigate the HetNets performance when comprised of full FD tier 2 and conventional HD tier 1. Therefore, using tools from stochastic geometry we present an analytical model for a two-tier HetNets, such that tier 1 comprises legacy HD macrocells while tier 2 consists of FD small cells, adopting flexible cell association. Specifically, the underlying model captures the downlink (DL) scenario for macrocell users, where the performance of the macrocell users is limited by several sources of interferences, such as other macrocell BSs, small cells, and other uplink (UL) small cell users, in addition to the DL scenarios of small cell users, where the performance of DL small cell users is limited by interferences such as macrocell BSs, other small cells, and other UL users. And finally, the UL small cell scenario, where the performance of the UL BS is limited by interferences such as macrocells, other small cells, UL small cell users and SI. We derive closed-form expressions for outage probability of the different tiers, and provide insights of performance with different parameters.

The rest of the paper is organized as follows. Section II provides the considered system model for the analysis in this paper. In Section III, we analyze the outage probability of two-tier HetNet with FD small cells. Numerical and simulation

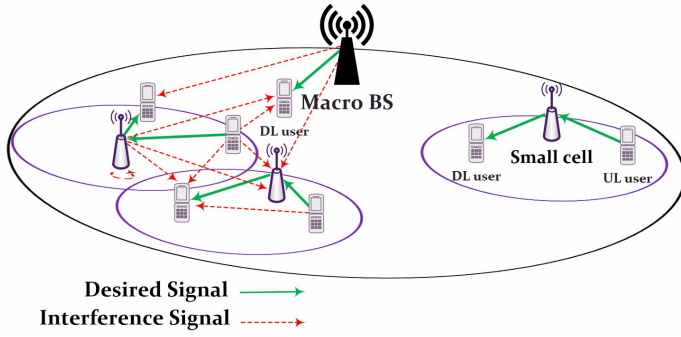


Fig. 1: Example cells of the system model, where macro BS operates in HD mode, and small cells operate in FD mode.

results are given in Section IV. Finally, concluding remarks and future work are provided in Section V.

II. SYSTEM MODEL

We consider a two-tier HetNets, where tier 1 comprises macro BSs operating in HD mode, and tier 2 consists of small cells operating in FD mode, as illustrated in Fig. 1. Both tiers are spatially distributed in \mathbb{R}^2 following homogeneous Poisson point processes (HPPPs) Φ_{S_1} and Φ_{S_2} , with intensities λ_{S_1} and λ_{S_2} , respectively. The UL small cell users are spatially located in \mathbb{R}^2 following the HPPP Φ_{U_2} , with intensity λ_{u_2} . Assuming that the intensity of DL users is high enough, and each user has data ready for transmission, such that saturated traffic conditions hold. We also assume that each small cell BS serves single active uplink user and single downlink user per channel, and each macrocell BS serves single active downlink user per channel. This assumption is justified due to the conclusions in [9], that the highest network performance is achieved when each tier in the network operates fully in either HD or FD, rather than having hybrid tiers. The full frequency reuse scenario is assumed, such that all the cells use the same frequency band. We assume that the channel coefficients are invariant in each block and vary between different blocks. Moreover, we assume that the channel $h_{i,j}$ between any pair of nodes i and j is impaired by Rayleigh fading.

We assume that the FD small cells are equipped with a single antenna and achieve FD capability through the techniques mentioned in [13]. A node in FD mode receives interference from its transmitted signal, and performs interference cancellation for that SI. Since the amount of SI depends on the transmission power at the receiver P_{S_2} , we define the residual self-interference (Δ) power after performing the SI cancellation as [9]

$$\Delta = P_{S_2} H_{SI} \quad (1)$$

In (1), $H_{SI} = |h_{SI}|^2$ is the residual SI channel gain of a tier 2 BS, indicating the SI cancellation capability of that BS, where h_{SI} is the SI channel of the BS. Note that $\Delta = 0$ denotes perfect cancellation capability. The residual SI channel gain H_{SI} is highly dependant on the adopted SI cancellation technique. For example, if digital-domain cancellation is

adopted, h_{SI} can be presented as $h_{SI} = h_{SI_c} - \hat{h}_{SI_c}$ where h_{SI_c} and \hat{h}_{SI_c} are the self-interfering channel and its estimate as the SI is subtracted using the estimate [9], [14]. With that, H_{SI} can be modeled as a constant value, such that $H_{SI} = \sigma_e^2$ for the estimation error variance σ_e^2 [9], [14]. On the other hand, using other cancellation techniques, makes modeling H_{SI} a challenging problem; hence, the parameter presented in (1) for the SI cancellation capability, can make the analysis more generic. Therefore, we consider H_{SI} to be a constant value. However, the analysis can still be extended to the case of random H_{SI} . For instance, once the probability density function (PDF) of H_{SI} is available for a certain SI cancellation mechanism, and by averaging the analytic results presented in this paper over the distribution of H_{SI} , the results for the random H_{SI} can be derived. This is beyond the scope of this paper and can be considered in future work.

We consider the maximum received power cell association rule in the downlink transmission of HetNets [10], such that, the association probability for the small cell \mathcal{A}_{S_2} and macrocell \mathcal{A}_{S_1} can be expressed as

$$\mathcal{A}_{S_2} = \mathbb{P}(P_{S_2}^r > P_{S_1}^r) = \left(1 + \frac{\lambda_{S_1}}{\lambda_{S_2}} \left(\frac{P_{S_1} h_{S_1}}{P_{S_2} h_{S_2}}\right)^{2/\alpha_1}\right)^{-1}, \quad (2)$$

$$\mathcal{A}_{S_1} = 1 - \mathcal{A}_{S_2} = 1 - \left(1 + \frac{\lambda_{S_1}}{\lambda_{S_2}} \left(\frac{P_{S_1} h_{S_1}}{P_{S_2} h_{S_2}}\right)^{2/\alpha_2}\right)^{-1}, \quad (3)$$

where $P_{S_1}^r$ and $P_{S_2}^r$ are the received power at the associating user from the macrocell and small cell BSs, respectively, h_{S_1} and h_{S_2} are the fading channel coefficients between the associated user with macrocell and small cell BSs, respectively. Moreover, α_1 and α_2 are the path loss exponents of macrocells and small cells, respectively.

A. Downlink SINR of Macrocell User

For a typical macrocell downlink user located at the origin u_1^0 , associated with its serving macrocell BS S_1^* , the SINR is expressed as

$$\text{SINR}_{u_1}^{DL} = \frac{P_{S_1} |h_{S_1^*, u_1^0}|^2 R_{S_1^*, u_1^0}^{-\alpha_1}}{I_{u_2}^{UL} + I_{S_2} + I_{S_1}^{DL} + N_0}, \quad (4)$$

where

$$\begin{aligned} I_{u_2}^{UL} &= \sum_{u_2 \in \Phi_{U_2}} P_{u_2} |h_{u_2, u_1^0}|^2 R_{u_2, u_1^0}^{-\alpha_2} \\ I_{S_2} &= \sum_{S_2 \in \Phi_{S_2}} P_{S_2} |h_{S_2, u_1^0}|^2 R_{S_2, u_1^0}^{-\alpha_2} \\ I_{S_1}^{DL} &= \sum_{S_1 \in \Phi_{S_1}} P_{S_1} |h_{S_1, u_1^0}|^2 R_{S_1, u_1^0}^{-\alpha_1}, \end{aligned}$$

given $I_{u_2}^{UL}$ is the interference from small cell uplink users, I_{S_2} is the interference from small cell BSs and $I_{S_1}^{DL}$ is the interference from other macrocell BSs.

In (4), P_{u_2} denotes the transmission power of small cell uplink users. Further, $h_{S_1^*, u_1^0}$, h_{u_2, u_1^0} , h_{S_2, u_1^0} , and h_{S_1, u_1^0} denote

the small scale fading channel coefficient for the channels of the typical downlink user and its serving macrocell BS, small cell users, small cell BSs and other non-associated macrocell BSs, respectively. Moreover, $R_{S_1^*, u_1^0}$, R_{u_2, u_1^0} , R_{S_2, u_1^0} , and R_{S_1, u_1^0} denote the distances between the typical downlink macrocell user and its associated macrocell BS, small cell users, small cell BSs, and other interfering macrocell BSs, respectively.

B. Downlink SINR of Small Cell User

For a typical small cell downlink user located at the origin u_2^0 , associated with its serving small cell BS S_2^* , the SINR expression is given by

$$SINR_{u_2}^{DL} = \frac{P_{S_2} |h_{S_2^*, u_2^0}|^2 R_{S_2^*, u_2^0}^{-\alpha_2}}{I_{u_2}^{UL} + I_{S_2} + I_{S_1}^{DL} + N_0}, \quad (5)$$

where

$$\begin{aligned} I_{u_2}^{UL} &= \sum_{u_2 \in \Phi_{U_2}} P_{u_2} |h_{u_2, u_2^0}|^2 R_{u_2, u_2^0}^{-\alpha_2} \\ I_{S_2} &= \sum_{S_2 \in \Phi_{S_2}} P_{S_2} |h_{S_2, u_2^0}|^2 R_{S_2, u_2^0}^{-\alpha_2} \\ I_{S_1}^{DL} &= \sum_{S_1 \in \Phi_{S_1}} P_{S_1} |h_{S_1, u_2^0}|^2 R_{S_1, u_2^0}^{-\alpha_1}, \end{aligned}$$

given $I_{u_2}^{UL}$ is the interference from small cell uplink users, I_{S_2} is the interference from small cell BSs and $I_{S_1}^{DL}$ is the interference from other macrocell BSs.

In (5), $h_{S_2^*, u_2^0}$, h_{u_2, u_2^0} , h_{S_2, u_2^0} , and h_{S_1, u_2^0} denote the small scale fading channel coefficient for the channels of the downlink typical small cell user and its serving small cell BS, small cell users, small cell BSs and macrocell BSs, respectively. Further, $R_{S_2^*, u_2^0}$, R_{u_2, u_1^0} , R_{S_2, u_1^0} , and R_{S_1, u_1^0} denote the distances between the typical small cell downlink user and its associated small cell BS, small cell users, other interfering small cell BSs, and macrocell BSs, respectively.

C. Uplink SINR of Small Cell BS

For a typical small cell BS in the uplink located at the origin S_2^0 , the SINR can be expressed as

$$SINR_{S_2}^{UL} = \frac{P_{u_2} |h_{u_2^*, S_2^0}|^2 R_{u_2^*, S_2^0}^{-\alpha_2}}{\Delta + I_{u_2}^{UL} + I_{S_2} + I_{S_1}^{DL} + N_0}, \quad (6)$$

where

$$\begin{aligned} I_{u_2}^{UL} &= \sum_{u_2 \in \Phi_{U_2}} P_{u_2} |h_{u_2, S_2^0}|^2 R_{u_2, S_2^0}^{-\alpha_2} \\ I_{S_2} &= \sum_{S_2 \in \Phi_{S_2}} P_{S_2} |h_{S_2, S_2^0}|^2 R_{S_2, S_2^0}^{-\alpha_2} \\ I_{S_1}^{DL} &= \sum_{S_1 \in \Phi_{S_1}} P_{S_1} |h_{S_1, S_2^0}|^2 R_{S_1, S_2^0}^{-\alpha_1}, \end{aligned}$$

given $I_{u_2}^{UL}$ denotes the interference from other small cell uplink users, I_{S_2} is the interference from other small cell BSs and $I_{S_1}^{DL}$ is the interference from macrocell BSs.

In (6), $h_{u_2^*, S_2^0}$, h_{u_2, S_2^0} , h_{S_2, S_2^0} , and h_{S_1, S_2^0} denote the small scale fading channel coefficient for the channels of small cell uplink BS and its associated small cell uplink user, other interfering small cell uplink users, other small cell BSs and macrocell BSs, respectively. Moreover, $R_{u_2^*, S_2^0}$, R_{u_2, S_2^0} , R_{S_2, S_2^0} , and R_{S_1, S_2^0} denote the distances between the typical small cell uplink BS and its associated small cell uplink user, other interfering small cell uplink users, other small cell BSs and macrocell BSs, respectively.

III. PERFORMANCE EVALUATION

In this section, we analyze the outage probability of two-tier HetNets with FD small cells, which is a metric that represents the average fraction of the cell area that is in outage at any time. We define the outage probability \mathbb{O} as the probability that the instantaneous SINR of a randomly located user is less than a target SINR τ . Since the typical user is associated with at most one tier, from the law of total probability, the outage probability is given as

$$\mathbb{O} = \sum_{k=1}^K \mathbb{O}_k \mathcal{A}_k, \quad (7)$$

where \mathcal{A}_k is the per-tier association probability given in (2) and (3), and \mathbb{O}_k is the outage probability of a typical user associated with k_{th} tier. For a target SINR τ_k and a typical user $SINR_k(x)$ at a distance x from its associated BS, the outage probability is given by

$$\mathbb{O}_k = \mathbb{E} [\mathbb{P} [SINR_k(x) < \tau_k]]. \quad (8)$$

Considering the chosen network model of HD macrocells and FD small cells, the expression of the outage probability becomes

$$\mathbb{O} = \mathbb{O}_1^{DL} \mathcal{A}_1 + (\mathbb{O}_2^{DL} + \mathbb{O}_2^{UL}) \mathcal{A}_2, \quad (9)$$

where \mathbb{O}_1^{DL} , \mathbb{O}_2^{DL} and \mathbb{O}_2^{UL} denote the outage probability of macrocell downlink user, smallcell downlink user, and small cell uplink BS, respectively, and are derived in the following section.

A. Outage Probability of Macrocell Downlink User

The probability density function (PDF) of the shortest distance between the typical macrocell user and the associated macrocell BS $R_{S_1^*, u_1^0}$, is given by

$$f_{R_{S_1^*, u_1^0}}(r) = \frac{2\pi\lambda_{S_1}}{\mathcal{A}_{S_1}} r \exp \left\{ -\pi \sum_{j=1}^2 \lambda_j \left(\frac{P_{S_j}}{P_{S_1}} \right)^{\frac{2}{\alpha_j/\alpha_1}} \right\}, \quad (10)$$

where \mathcal{A}_{S_1} is given in (3).

Theorem 1. The outage probability \mathbb{O}_1^{DL} is defined as the probability that the instantaneous SINR of a randomly located macrocell downlink user is lower than a target τ_1 , is given by

$$\mathbb{O}_1^{DL} = 1 - \left\{ \frac{2\pi\lambda_{S_1}}{\mathcal{A}_{S_1}} \int_0^\infty r \exp \left\{ -r^{\alpha_1} P_{S_1}^{-1} N_0 \tau_1 - \pi \left((\Psi_1 r^{\frac{2}{\alpha_2}}) + (\Psi_2 r^{\frac{2}{\alpha_2}}) + (\Psi_3 r^2) \right) \right\} dr \right\}. \quad (11)$$

given,

$$\begin{aligned} \Psi_1 &= \lambda_{u_2} \left(\frac{P_{u_2}}{P_{S_1}} \right)^{2/\alpha_2} \frac{2\tau_1}{\alpha_2 - 2} {}_2F_1 \left[1, 1 - \frac{2}{\alpha_2}; 2 - \frac{2}{\alpha_2}; -\tau_1 \right], \\ \Psi_2 &= \lambda_{S_2} \left(\frac{P_{S_2}}{P_{S_1}} \right)^{2/\alpha_2} \frac{2\tau_1}{\alpha_2 - 2} {}_2F_1 \left[1, 1 - \frac{2}{\alpha_2}; 2 - \frac{2}{\alpha_2}; -\tau_1 \right], \\ \Psi_3 &= \lambda_{S_1} \left(\frac{P_{S_1}}{P_{S_1}^*} \right)^{2/\alpha_1} \frac{2\tau_1}{\alpha_1 - 2} {}_2F_1 \left[1, 1 - \frac{2}{\alpha_1}; 2 - \frac{2}{\alpha_1}; -\tau_1 \right]. \end{aligned}$$

where ${}_2F_1[\cdot]$ denote the Gauss hypergeometric function, and the pathloss exponents $\alpha_j > 2$.

Proof. See Appendix A ■

B. Outage Probability of Tier 2 Downlink User

The PDF of the shortest distance between the typical small cell downlink user and the associated BS $R_{S_2^*, u_2^0}$, is given by

$$f_{R_{S_2^*, u_2^0}}(r) = \frac{2\pi\lambda_{S_2}}{\mathcal{A}_{S_2}} r \exp \left\{ -\pi \sum_{j=1}^2 \lambda_j (P_{S_j} / P_{S_2})^{\frac{2}{\alpha_j}} \right\}. \quad (12)$$

where \mathcal{A}_{S_2} is given in (2)

Theorem 2. The outage probability \mathbb{O}_2^{DL} is defined as the probability that the instantaneous SINR of a randomly located small cell downlink user is lower than a target τ_2 is given by

$$\mathbb{O}_2^{DL} = 1 - \left\{ \frac{2\pi\lambda_{S_2}}{\mathcal{A}_{S_2}} \int_0^\infty r \exp \left\{ -r^{\alpha_2} P_{S_2}^{-1} N_0 \tau_2 - \pi \left((\eta_1 r^2) + (\eta_2 r^{\frac{2}{\alpha_2}}) + (\eta_3 r^{\frac{2}{\alpha_1}}) \right) \right\} dr \right\}, \quad (13)$$

given,

$$\begin{aligned} \eta_1 &= \lambda_{u_2} \left(\frac{P_{u_2}}{P_{S_2}} \right)^{2/\alpha_2} \frac{2\tau_2}{\alpha_2 - 2} {}_2F_1 \left[1, 1 - \frac{2}{\alpha_2}; 2 - \frac{2}{\alpha_2}; -\tau_2 \right], \\ \eta_2 &= \lambda_{S_2} \left(\frac{P_{S_2}}{P_{S_2}^*} \right)^{2/\alpha_2} \frac{2\tau_2}{\alpha_2 - 2} {}_2F_1 \left[1, 1 - \frac{2}{\alpha_2}; 2 - \frac{2}{\alpha_2}; -\tau_2 \right], \\ \eta_3 &= \lambda_{S_1} \left(\frac{P_{S_1}}{P_{S_2}} \right)^{2/\alpha_1} \frac{2\tau_2}{\alpha_1 - 2} {}_2F_1 \left[1, 1 - \frac{2}{\alpha_1}; 2 - \frac{2}{\alpha_1}; -\tau_2 \right]. \end{aligned}$$

where the pathloss exponents $\alpha_j > 2$.

Proof. Following the derivation approach presented in Appendix A, the final expression for the outage probability of a randomly located small cell DL user is given in (13). ■

TABLE I: Parametric Values (unless otherwise specified)

Parameter	Value
$\lambda_x \forall x$	$(\pi \times 500^2)^{-1}$
P_{S_1} [dBm]	46 dBm
P_{S_2} [dBm]	26 dBm
$P_{u_y} \forall y$ [dBm]	26 dBm
W [Hz]	10^4
$\alpha_k \forall k$	4
$\tau_n \forall n$ [dB]	0 dB
Δ	$P_{S_2} 10^{L_{dB}/10}$
L_{dB} [dB]	-38 dB

C. Outage Probability of Tier 2 Uplink BS

The SINR of an uplink small cell BS is given in (6).

Theorem 3. The outage probability \mathbb{O}_2^{UL} is defined as the probability that the instantaneous SINR of a randomly located small cell uplink BS is lower than a target τ_3 is given by

$$\mathbb{O}_2^{UL} = 1 - \left\{ \frac{2\pi\lambda_{u_2}}{\mathcal{A}_{S_2}} \int_0^\infty r \exp \left\{ -r^{\alpha_2} P_{u_2}^{-1} P_{S_2} \sigma_e^2 N_0 \tau_3 - \pi \left((\Gamma_1 r^2) + (\Gamma_2 r^2) + (\Gamma_3 r^{\frac{2}{\alpha_1}}) \right) \right\} dr \right\}. \quad (14)$$

given,

$$\begin{aligned} \Gamma_1 &= \lambda_{u_2} \left(\frac{P_{u_2}}{P_{u_2}} \right)^{2/\alpha_2} \frac{2\tau_3}{\alpha_2 - 2} {}_2F_1 \left[1, 1 - \frac{2}{\alpha_2}; 2 - \frac{2}{\alpha_2}; -\tau_3 \right], \\ \Gamma_2 &= \lambda_{S_2} \left(\frac{P_{S_2}}{P_{u_2}} \right)^{2/\alpha_2} \frac{2\tau_3}{\alpha_2 - 2} {}_2F_1 \left[1, 1 - \frac{2}{\alpha_2}; 2 - \frac{2}{\alpha_2}; -\tau_3 \right], \\ \Gamma_3 &= \lambda_{S_1} \left(\frac{P_{S_1}}{P_{u_2}} \right)^{2/\alpha_1} \frac{2\tau_3}{\alpha_1 - 2} {}_2F_1 \left[1, 1 - \frac{2}{\alpha_1}; 2 - \frac{2}{\alpha_1}; -\tau_3 \right], \end{aligned}$$

where the pathloss exponents $\alpha_j > 2$.

Proof. From (8), The outage probability \mathbb{O}_2^{UL} can be obtained by (15)

$$\mathbb{O}_2^{UL} = \mathbb{E} \left[\mathbb{P} [SINR_{S_2}^{UL} < \tau_3] \right]. \quad (15)$$

Following similar approach used to prove the aforementioned theorems, the outage probability of an UL small cell BS is given by (14). This completes the proof. ■

IV. NUMERICAL RESULTS

In this section, we evaluate the performance of two-tier HetNets with FD small cells. We investigate how tier 2 density and the SI cancellation capabilities affect the outage probability. The parameters used for the analysis and simulation are presented in Table I. Monte Carlo simulations have been performed to verify our derived analytical results by averaging over 10000 iterations.

Fig. 2 plots the outage probability of a typical DL user associated with macrocell BS, small cell BS, and random type of BS in the DL, as a function of small cell BSs density λ_2 . We observe that outage probability of macrocell DL user increases with increasing the small cell BS density. This results from the increase in aggregate interference from the small

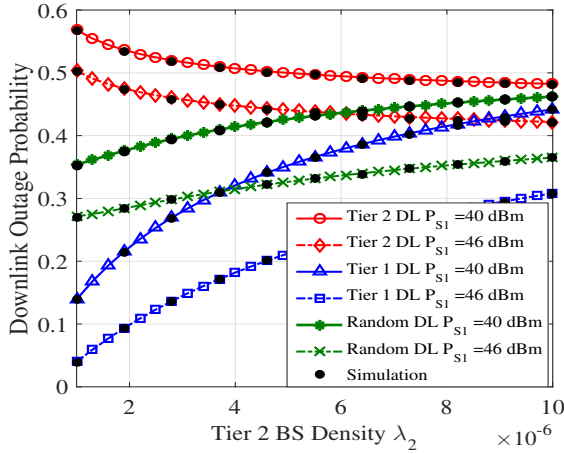


Fig. 2: Outage probability of tier 1 and tier 2 downlink as a function of tier 2 density λ_2 .

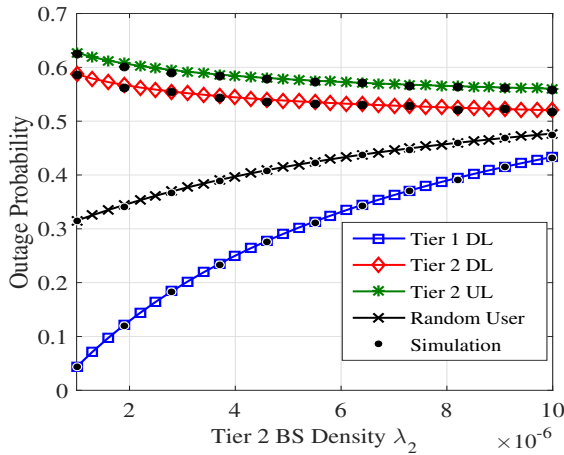


Fig. 3: Outage probability as a function of tier 2 density λ_2 .

cell BSs, as shown in (4). Additionally, outage probability of macrocell DL user decreases with increasing the transmit power at the macrocell BS, which is due to the increase in SINR at the typical downlink user associated with macrocell BS, as shown in (4). Interestingly, for the typical downlink user associated with small cell BS, the outage probability decrease with increasing the small cell BS density. This is because densification of tier 2 reduces the inter-link distances between the typical downlink user and the associated small cell BS, as shown in (5). In addition, outage probability of typical small cell DL user decrease with increasing the transmit power at the macrocell BS, which is due to the increase in aggregate interference caused by macrocell BSs, as shown in (5). Finally, outage probability of a random DL user, which is defined as $\mathbb{O}_1^{DL} \mathcal{A}_1 + \mathbb{O}_2^{DL} \mathcal{A}_2$, increases with both the increase of small cell density, and the decrease of transmit power of macrocell BS. This is because \mathbb{O}_1^{DL} in the expression is lower than \mathbb{O}_2^{DL} , therefore the expression reflects such tendency.

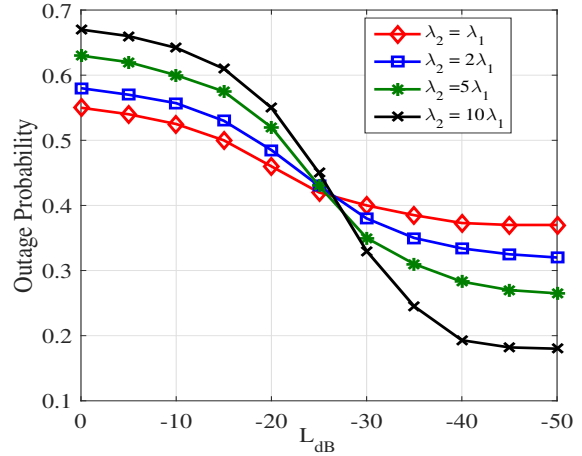


Fig. 4: Outage probability as a function of the SI cancellation capability L_{dB} .

Fig. 3 plots the outage probability of macrocell DL user, small cell DL user, small cell UL BS, and a randomly located user, against density of small cell BSs. In this figure, we focus on the impact of small cell BSs density on outage probability of a randomly located user. We observe that outage probability of a randomly located user increases with increasing the small cell BS density. This results from the increase in aggregate interference from the small cell BSs, as shown in (9).

Fig. 4 plots the relation between outage probability and SI cancellation capability L_{dB} . We observe that outage probability of a randomly located user is initially high, especially when SI cancellation capability is low ($L_{dB} < -15$), then it decreases with increasing L_{dB} , until it nearly stabilise beyond ($L_{dB} > -37$). This is because high SI cancellation capabilities improve the performance of FD links as can be seen in (6). Additionally, we observe that the outage probability in high small cell densities is more sensitive to L_{dB} variations. This due to increased FD links in higher small cell densities since only the small cell BSs operate in FD mode.

V. CONCLUSION AND FUTURE WORK

Realizing the FD capability at small cells is particularly attractive due to cost efficiency, ease of deployment, and higher SI cancellation capabilities (compared to macrocells). In this paper, we have investigated the performance of two-tier HetNets with FD small cells. We have derived the closed-form expressions for outage probability in two-tier HetNets with FD small cells. Our performance evaluation investigates the impact of different network parameters on outage probability. The results demonstrate that the HetNets achieves lower outage with higher densities of FD small cells. Moreover, as expected, the outage probability improves with higher SI cancellation capabilities. Additional work on the selected system model can be investigated, exploring different metrics, e.g. rate coverage probability, sum ergodic rate and throughput. Additionally, considering different inter-cell coordination schemes can be accounted for, which makes HetNet analysis more realistic.

A. Proof of Theorem 1.

From (8), the outage probability \mathbb{O}_1^{DL} is given as

$$\begin{aligned}\mathbb{O}_1^{DL} &= \mathbb{E} \left[\mathbb{P} \left[SINR_{u_1}^{DL} < \tau_1 \right] \right] \\ &= 1 - \int_0^\infty \mathbb{P} \left[SINR_{u_1}^{DL} > \tau_1 \right] f_{R_{S_1^*, u_1^0}}(r) dr \\ &= 1 - \frac{2\pi\lambda_{S_1}}{\mathcal{A}_{S_1}} \int_0^\infty \mathbb{P} \left[SINR_{u_1}^{DL} > \tau_1 \right] r \\ &\quad \times \exp \left\{ -\pi \sum_{j=1}^2 \lambda_j \left(\frac{P_{S_j}}{P_{S_1}} \right)^{\zeta_1} r^{\zeta_1} \right\} dr, \quad (16)\end{aligned}$$

where $\zeta_1 = \frac{2}{\alpha_j/\alpha_1}$. By setting $Q_1 = I_{u_2}^{UL} + I_{S_2} + I_{S_1}^{DL} + N_0$, We rewrite $\mathbb{P} \left[SINR_{u_1}^{DL} > \tau_1 \right]$ as

$$\begin{aligned}\mathbb{P} \left[SINR_{u_1}^{DL} > \tau_1 \right] &= \mathbb{P} \left[h_{S_1, u_1} > P_{S_1}^{-1} r^{\alpha_1} \tau_1 Q_1 \right] \\ &= \exp \left\{ -r^{\alpha_1} P_{S_1}^{-1} N_0 \tau_1 \right\} \mathcal{L}_{I_{u_2}^{UL}}(r^{\alpha_1} P_{S_1}^{-1} \tau_1) \\ &\quad \times \mathcal{L}_{I_{S_2}}(r^{\alpha_1} P_{S_1}^{-1} \tau_1) \mathcal{L}_{I_{S_1}^{DL}}(r^{\alpha_1} P_{S_1}^{-1} \tau_1). \quad (17)\end{aligned}$$

Starting with the Laplace transform of the interference originated from other small cell UL users in (17), we have

$$\begin{aligned}\mathcal{L}_{I_{u_2}^{UL}}(r^{\alpha_1} P_{S_1}^{-1} \tau_1) &= \mathbb{E}_{I_{u_2}^{UL}} \left[\exp \left\{ -r^{\alpha_1} P_{S_1}^{-1} \tau_1 I_{u_2}^{UL} \right\} \right] \\ &= \mathbb{E}_{\Phi_{U_2}} \left[\exp \left\{ -r^{\alpha_1} \frac{P_{u_2}}{P_{S_1}} \tau_1 \sum_{u_2 \in \Phi_{U_2}} h_{u_2, u_1^0} R_{u_2, u_1^0}^{-\alpha_2} \right\} \right] \\ &= \exp \left\{ -2\pi\lambda_{u_2} \int_0^\infty 1 - \mathcal{L}_{h_{S_1, u_1}} \left(r^{\alpha_1} \frac{P_{u_2}}{P_{S_1}} \tau_1 x^{-\alpha_2} \right) x dx \right\} \\ &= \exp \left\{ -2\pi\lambda_{u_2} \int_0^\infty \frac{x}{1 + \left(r^{\alpha_1} \frac{P_{u_2}}{P_{S_1}} \tau_1 \right)^{-1} x^{\alpha_2}} dx \right\}. \quad (18)\end{aligned}$$

Note that the integration limits in (18) are from 0 to ∞ since the small cell UL users can be at any distance from the DL macrocell users. Now, with a change of variables $v_1 = \left(r^{\alpha_1} \frac{P_{u_2}}{P_{S_1}} \tau_1 \right)^{-2/\alpha_2} x^2$, We express

$$\begin{aligned}\mathcal{L}_{I_{u_2}^{UL}}(r^{\alpha_1} P_{S_1}^{-1} \tau_1) &= \exp \left\{ -\pi\lambda_{u_2} \left(\frac{P_{u_2}}{P_{S_1}} \right)^{2/\alpha_2} \right. \\ &\quad \left. \times Z_1(\tau_1, \alpha_2) r^{\frac{2}{\alpha_2/\alpha_1}} \right\}, \quad (19)\end{aligned}$$

where

$$\begin{aligned}Z_1(\tau_1, \alpha_2) &= \tau_1^{2/\alpha_2} \int_{x_1}^\infty \frac{1}{1 + v_1^{\alpha_2/2}} dv_1 \\ &= \frac{2\tau_1}{\alpha_2 - 2} {}_2F_1[1, 1 - 2/\alpha_2; 2 - 2/\alpha_2; -\tau_1]. \quad (20)\end{aligned}$$

In (20), ${}_2F_1[\cdot]$ denote the Gauss hypergeometric function and $x_1 = (1/\tau_1)^{2/\alpha_2}$. The expression holds for $\alpha_2 > 2$.

Similarly, we can derive the Laplace transform for the interference from small cells BSs expressed in (17), as

$$\begin{aligned}\mathcal{L}_{I_{S_2}}(r^{\alpha_1} P_{S_1}^{-1} \tau_1) &= \exp \left\{ -\pi\lambda_{S_2} (P_{S_2}/P_{S_1})^{2/\alpha_2} \right. \\ &\quad \left. \times \frac{2\tau_1}{\alpha_2 - 2} {}_2F_1[1, 1 - 2/\alpha_2; 2 - 2/\alpha_2; -\tau_1] \right\}, \quad (21)\end{aligned}$$

for $\alpha_2 > 2$. We finally derive the Laplace transform for the interference originated from macrocell BSs expressed in (17) using similar approach, as

$$\begin{aligned}\mathcal{L}_{I_{S_1}^{DL}}(r^{\alpha_1} P_{S_1}^{-1} \tau_1) &= \exp \left\{ -\pi\lambda_{S_1} (P_{S_1}/P_{S_1}^*)^{2/\alpha_1} \right. \\ &\quad \left. \times \frac{2\tau_1}{\alpha_1 - 2} {}_2F_1[1, 1 - 2/\alpha_1, -\tau_1] \right\}, \quad (22)\end{aligned}$$

for $\alpha_1 > 2$. Now, plugging (19), (21) and (22) into $\mathbb{P} \left[SINR_{u_1}^{DL} > \tau_1 \right]$ we obtain (23),

$$\begin{aligned}\mathbb{P} \left[SINR_{u_1}^{DL} > \tau_1 \right] &= \exp \left\{ -r^{\alpha_1} P_{S_1}^{-1} N_0 \tau_1 \right. \\ &\quad \left. - \pi \left(\left(\Psi_1 r^{\frac{2}{\alpha_2/\alpha_1}} \right) + \left(\Psi_2 r^{\frac{2}{\alpha_2/\alpha_1}} \right) + \left(\Psi_3 r^2 \right) \right) \right\}. \quad (23)\end{aligned}$$

given

$$\begin{aligned}\Psi_1 &= \lambda_{u_2} \left(\frac{P_{u_2}}{P_{S_1}} \right)^{2/\alpha_2} \frac{2\tau_1}{\alpha_2 - 2} {}_2F_1[1, 1 - 2/\alpha_2; 2 - 2/\alpha_2; -\tau_1], \\ \Psi_2 &= \lambda_{S_2} \left(\frac{P_{S_2}}{P_{S_1}} \right)^{2/\alpha_2} \frac{2\tau_1}{\alpha_2 - 2} {}_2F_1[1, 1 - 2/\alpha_2; 2 - 2/\alpha_2; -\tau_1], \\ \Psi_3 &= \lambda_{S_1} \left(\frac{P_{S_1}}{P_{S_1}^*} \right)^{2/\alpha_1} \frac{2\tau_1}{\alpha_1 - 2} {}_2F_1[1, 1 - 2/\alpha_1; 2 - 2/\alpha_2; -\tau_1],\end{aligned}$$

where $\alpha_j > 2$. Therefore, the final expression for a randomly located macrocell DL user is given by (11).

REFERENCES

- [1] A. Goldsmith, *Wireless communications*. Cambridge university press, 2005.
- [2] M. Duarte, C. Dick, and A. Sabharwal, "Experiment-driven characterization of full-duplex wireless systems," *IEEE Trans. Wireless Commun.*, vol. 11, no. 12, pp. 4296–4307, May 2012.
- [3] D. Bharadia, E. McMillin, and S. Katti, "Full duplex radios," *SIGCOMM Comput. Commun. Rev.*, vol. 43, no. 4, pp. 375–386, Aug 2013.
- [4] M. Duarte, A. Sabharwal, V. Aggarwal, R. Jana, K. Ramakrishnan, C. W. Rice, and N. Shankaranarayanan, "Design and characterization of a full-duplex multiantenna system for wifi networks," *IEEE Trans. Veh. Technol.*, vol. 63, no. 3, pp. 1160–1177, Nov 2014.
- [5] J. I. Choi, M. Jain, K. Srinivasan, P. Levis, and S. Katti, "Achieving single channel, full duplex wireless communication," *ACM MobiCom*, pp. 1–12, Sep 2010.
- [6] J. G. Andrews, "Seven ways that hetnets are a cellular paradigm shift," *IEEE Commun. Mag.*, vol. 51, no. 3, pp. 136–144, Mar 2013.
- [7] V. Chandrasekhar, J. G. Andrews, and A. Gatherer, "Femtocell networks: a survey," *IEEE Commun. Mag.*, vol. 46, no. 9, pp. 59–67, Sep 2008.
- [8] M. Al-Kadri, A. Aijaz, and A. Nallanathan, "Ergodic capacity of interference coordinated hetnet with full-duplex small cells," *EW*, pp. 1–6, May 2015.
- [9] J. Lee and T. Quek, "Hybrid full/half-duplex system analysis in heterogeneous wireless networks," *IEEE Trans. Wireless Commun.*, vol. 14, no. 5, pp. 2883–2895, May 2015.
- [10] H.-S. Jo, Y. J. Sang, P. Xia, and J. Andrews, "Heterogeneous cellular networks with flexible cell association: A comprehensive downlink sinr analysis," *IEEE Trans. Wireless Commun.*, vol. 11, no. 10, Oct 2012.
- [11] H. Tabassum, A. H. Sakr, and E. Hossain, "Massive mimo-enabled wireless backhubs for full-duplex small cells," *IEEE GLOBECOM*, pp. 1–6, Dec 2015.
- [12] Z. Zhang, Z. Ma, Z. Ding, M. Xiao, and G. Karagiannidis, "Full-duplex two-way and one-way relaying: Average rate, outage probability and tradeoffs," *IEEE Trans. Wireless Commun.*, no. 99, p. 1, Feb 2016.
- [13] C. Cox and E. Ackerman, "Demonstration of a single-aperture, full-duplex communication system," in *IEEE RWS*, Jan 2013, pp. 148–150.
- [14] T. Riihonen, S. Werner, and R. Wichman, "Mitigation of Loopback Self-Interference in Full-Duplex MIMO Relays," *IEEE Trans. Signal Process.*, vol. 59, no. 12, pp. 5983–5993, Dec 2011.